ORNL/TM-9504
Dist. Category UC-20 g

ORNL/TM--9504

DE85 009671

Fusion Energy Division

A FLEXIBLE HELIAC CONFIGURATION

J. H. Harris
J. L. Cantrell*
T. C. Hender
B. A. Carreras
R. N. Morris*

*Computing and Telecommunications Division

Date Published - April 1985

Prepared by the
OAK RIDGE NATIONAL LABORATORY
Oak Ridge, Tennessee 37831
operated by
MARTIN MARIETTA ENERGY SYSTEMS, INC.
for the
U.S. DEPARTMENT OF ENERGY
under Contract No. DE-AC05-84OR21400

ACKNOWLEDGMENTS

We are grateful to J. A. Rome, V. E. Lynch, and J. Guasp for their help in carrying out the computations and to J. F. Lyon for continuing support and encouragement. In addition, one of us (J. H. H.) acknowledges a discussion of the results of Ref. [13] with S. Yoshikawa.

ABSTRACT

The addition of an $\ell = 1$ helical winding to the heliac central conductor adds a significant degree of flexibility to the configuration by making it possible to control the rotational transform and shear. Such control is essential for an experiment because the presence of low-order resonances in the rotational transform profile can cause breakup of the equilibrium magnetic surfaces. The use of the additional winding also permits reduction of the total central conductor current and can deepen the magnetic well.

Helical-axis stellarators with high rotational transform, low shear ($d\iota/dr \approx 0$), and an average magnetic well have been shown theoretically capable of stably confining plasmas with β greater than 10% in the infinite-aspect-ratio limit [1–4], and a relatively simple coil set — the heliac [4] — has been proposed as a finite-aspect-ratio realization of such a configuration. However, both analytic [5] and numerical [6,7] studies of finite-aspect-ratio, three-dimensional (3-D) equilibria have shown that the growth of finite plasma-pressure-induced field harmonics resonant at rational values of the rotational transform can lead to formation of large magnetic islands. These islands break up the equilibrium flux surfaces at low β values, which would presumably lead to a significant deterioration of confinement in an experiment. Similar effects have already been observed for $\beta \lesssim 1\%$ in the circular-axis, low-shear, Wendelstein VIIA device [8], which has a fairly low transform per period ($\iota/M \sim 0.1$). Heliac configurations typically have higher values of $\iota/M \gtrsim 0.3$; this greatly increases the number and strength of the potential low-order resonances [5,7,9]. It is important, therefore, to have a means of rotational transform profile control in an experimental heliac device in order to explore (and ultimately avoid) the dangerous resonances.

In this paper we show that the incorporation of an $\ell = 1$ helical winding into the hardcore of the heliac configuration (Fig. 1) introduces an extra degree of freedom that can be used to control the rotational transform profile; this technique could be valuable in both the design and operation of a heliac device. The additional winding can incidentally lead to a deepening of the magnetic well. This latter finding is in qualitative agreement with the physical reasoning in

ORNL–DWG 84-3803A FED

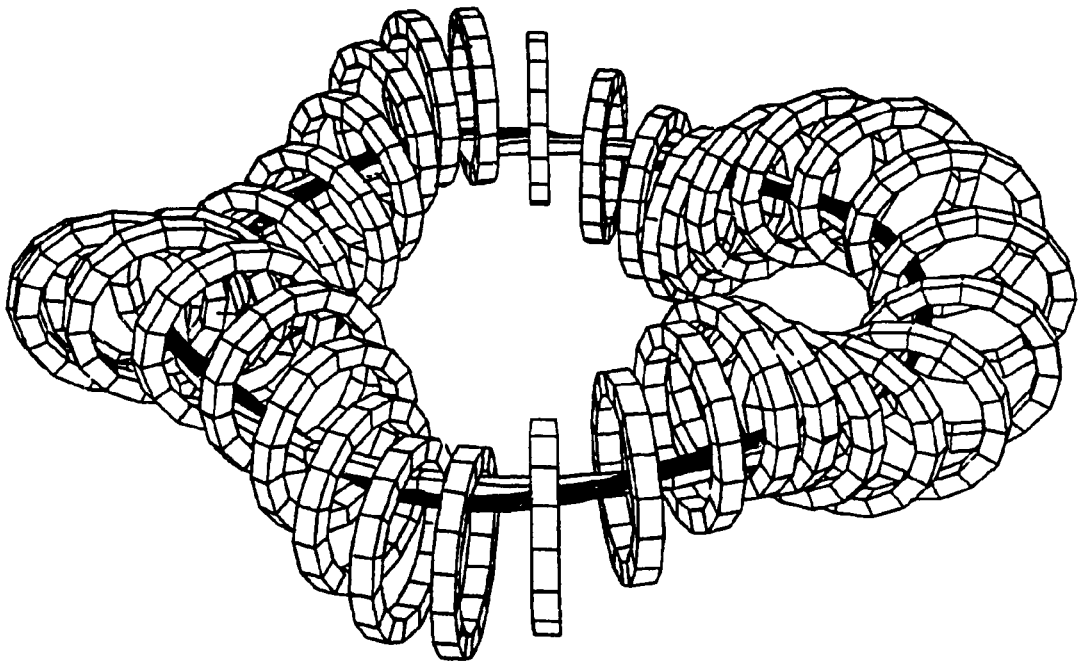

FIG. 1. Coil set for modified heliac configuration, showing additional $\ell = 1$ hardcore winding (shaded).

early papers [10–12] on this general type of configuration, as well as with a more recent calculation by Yoshikawa [13], who showed that an $\ell = 2$ hardcore could be used to produce a magnetic well in a heliac configuration that otherwise would not have $V'' < 0$ everywhere.

To elucidate some of the properties of the heliac with an $\ell = 1$ hardcore winding, it is useful to consider a simple analytic model. In the helically symmetric limit, the helical flux function is given by [10–12, 14]:

$$\psi = \frac{B_0}{R_0}\frac{r^2}{2} - \frac{\mu_0 I}{2\pi}\ln r - r\left[a_1 I_1'\left(\frac{r}{R_0}\right) + b_1 K_1'\left(\frac{r}{R_0}\right)\right]\cos\left(\theta - \frac{z}{R_0}\right), \quad (1)$$

where only the dominant helical terms are retained and I_1 and K_1 are modified Bessel functions. The first term in Eq. (1) represents a uniform toroidal field of strength B_0, while the second term results from the net longitudinal current I flowing in the central conductor and the unidirectional $\ell = 1$ hardcore winding. The I_1 and K_1 helical terms are due, respectively, to the "external" $\ell = 1$ field (which in a heliac is generated by the helical displacement of the toroidal field coils) and the "internal" $\ell = 1$ field of the helical hardcore.

The magnetic axis (0-point) is the turning point of Eq. (1) with $\theta = z/R_0$ and $r = r_A$, where

$$\frac{r_A}{R_0} - \frac{\mu_0 I}{2\pi R_0 B_0}\frac{R_0}{r_A} = \frac{R_0}{r_A}\left(\frac{r_A^2}{R_0^2} + 1\right)\left[\frac{a_1}{B_0} I_1\left(\frac{r_A}{R_0}\right) + \frac{b_1}{B_0} K_1\left(\frac{r_A}{R_0}\right)\right] . \qquad (2)$$

Expanding in a Taylor series about the magnetic axis, we find that the ellipticity of the magnetic surfaces is

$$e = \left\{ \frac{\partial^2\psi}{\partial r^2} \Big/ \left[\frac{1}{r_A^2}\frac{\partial^2\psi}{\partial\theta^2}\left(1 + \frac{r_A^2}{R_0^2}\right)\right]\right\}^{1/2} , \qquad (3)$$

where the second derivatives are evaluated at $r = r_A$. The $(1 + r_A^2/R_0^2)$ term in Eq. (3) occurs because we require the ellipticity to be in the plane normal to the magnetic axis. The ellipticity is directly related to the rotational transform per field period at the magnetic axis [12] by

$$\frac{\iota_0}{M} = 1 - \frac{2e}{e^2 + 1}\frac{1}{(1 + r_A^2/R_0^2)^{1/2}} . \qquad (4)$$

From Eqs. (1) and (3), we find

$$\frac{\mu_0 I}{2\pi R_0 B_0} = \frac{a_1 r_A}{4B_0 R_0}\left[\left(\frac{r_A^2}{R_0^2} + e^2 - 1\right) I_0\left(\frac{r_A}{R_0}\right) + \left(e^2 + 3 + \frac{r_A^2}{R_0^2}\right) I_2\left(\frac{r_A}{R_0}\right)\right]$$

$$- \frac{b_1 r_A}{4B_0 R_0}\left[\left(\frac{r_A^2}{R_0^2} + e^2 - 1\right) K_0\left(\frac{r_A}{R_0}\right) + \left(e^2 + 3 + \frac{r_A^2}{R_0^2}\right) K_2\left(\frac{r_A}{R_0}\right)\right] . \tag{5}$$

Given any three of the quantities I, a_1, b_1, e, and ι_0/M, the others may be determined from Eqs. (3) through (5). In examining Eq. (5), it is clear that, for a given a_1 and ellipticity (or equivalently ι_0), as b_1 increases, the required I decreases. Physically, this means that to maintain constant ι_0 we require less total current in the hardcore as the current in the helical hardcore is increased. There is a further effect that decreases the current I when b_1/B_0 increases. This is due to the change of magnetic axis position with b_1/B_0, as can be seen from Eq. (2). Figure 2 shows the reduction of the current I with b_1/B_0 for the particular parameters $a_1/B_0 = 0.25$ and $\iota_0/M = 0.3$. This figure shows both the variation in hardcore current I due to increasing b_1 and the variation in I due to the magnetic axis shift [Eq. (2)] alone. Also plotted in Fig. 2 are results from numerical field-line tracing calculations using the helical flux given by Eq. (1). The analytic and numerical results are in good agreement.

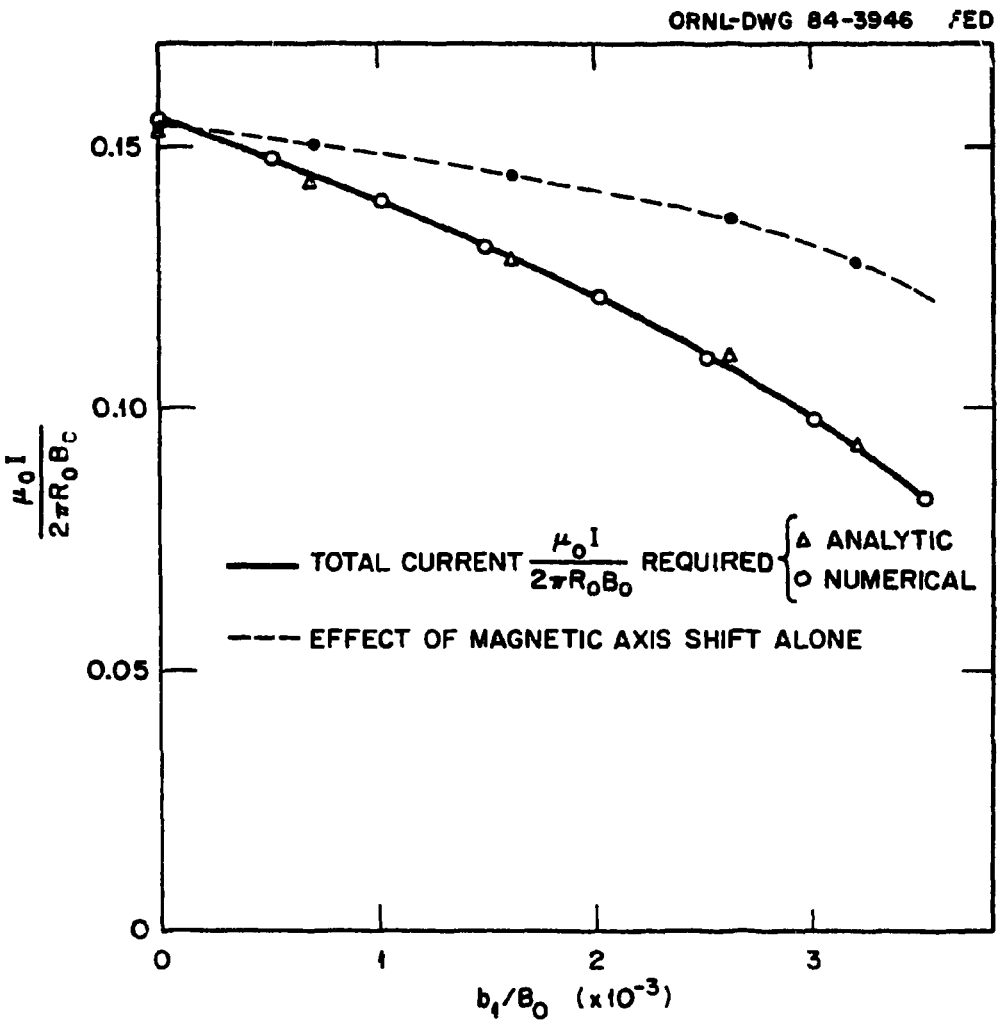

FIG. 2. For a helically symmetric field model, the net longitudinal hardcore current I required to maintain constant $\iota_0/M = 0.3$ decreases as the $\ell = 1$ helical hardcore field component b_1 is increased. For this example, $a_1/B_0 = 0.25$ in Eq. (1).

Using the expressions given in Ref. [12], we can also compute V'' at the magnetic axis:

$$V'' = \frac{2}{R_0 B_0^2 e^2 (1 + r_A^2/R_0^2)^{3/2}}$$

$$\times \left[\frac{r_A^2}{R_0^2} - \frac{e^2 - 1 - r_A^2/R_0^2}{1 + r_A^2/R_0^2} \left(\frac{R_0}{2r_A} \frac{a_1 I_1 + b_1 K_1}{a_1 I_1' + b_1 K_1'} - \frac{1 + r_A^2/R_0^2}{e^2 + 1 + r_A^2/R_0^2} \right) \right] . \quad (6)$$

For the same parameters as in Fig. 2, this expression gives $R_0 B_0^2 V'' = -0.197$ when $b_1/B_0 = 0$, and $R_0 B_0^2 V'' = -0.497$ when $b_1/B_0 = 3.2 \times 10^{-3}$. Thus, for a fixed ι_0 the magnetic well gets deeper as the current in the helical hardcore is raised. Numerical field-tracing calculations also show the same result.

We have found that while helically symmetric calculations are useful as a general guide to the behavior of the central transform and magnetic well, full 3-D calculations using a filamentary representation of the heliac coil set are necessary to accurately determine flux surface shapes and profiles of transform and V''. This is because the existence and shape of magnetic surfaces are strongly affected by (1) the finite extent of the toroidal coils and (2) toroidal effects (which actually determine the last closed surface by introducing resonances [15]). In the calculations that follow, we represent a heliac configuration as an array of N circular coils of radius a_c, whose centers are located on a toroidal helix having major radius R_0, minor radius r_{SW}, and M periods. For all of the calculations shown here, N/M = 9 coils per period. The nominal toroidal field strength is given

(in amperes per meter) by $H_0 = NI_{TF}/2\pi R_0$, where I_{TF} is the toroidal field coil current. The circular center conductor at the minor axis carries a current I_R. The helical hardcore winding carries a current I_{H1} and follows the same winding law ($\theta = M\phi$) as do the toroidal field coils, but with a minor radius a_{hc} ($< a_c$). The total (toroidally directed) current in the hardcore is $I_T = I_R + I_{H1}$. A small external vertical field of about 5% of H_0 is required to define the magnetic axis, which we usually shift toroidally outward (relative to the "helically centered" position) by a small amount ($\Delta R/R_0 \sim 1\%$) to improve the magnetic well and flux surface size.

Figure 3 shows the results of 3-D field-line calculations for two heliac configurations — one with a helical hardcore winding and one without. The two configurations are essentially identical in rotational transform profile and average last closed-surface radius, but the configuration with the helical hardcore winding requires somewhat less than one-half the total toroidal hardcore current [i.e., one-half the value of $I_T/(R_0H_0)$]. This is in good agreement with the analytical calculations done in the helically symmetric limit. The profiles of V' from the field-line calculations show that the configuration with the helical hardcore has a deeper magnetic well, as is also indicated by the greater indentation in the magnetic surface shape. The increase in magnetic well is in agreement with the analytic calculations. Figure 4 shows how the axis position varies as a function of helical hardcore current for the same configuration as in Fig. 3. This also shows good agreement with the analytic calculations: the axis shifts helically inward (toward the hardcore) as the fraction of the current flowing in the helical winding increases.

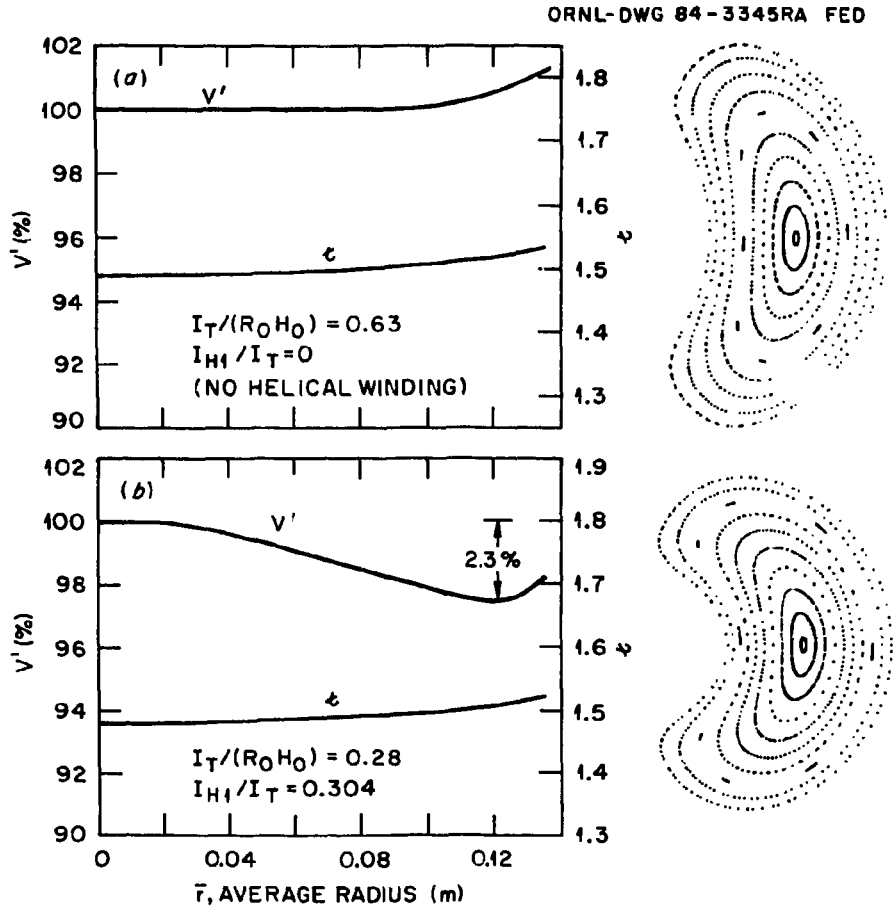

FIG. 3. Comparison of ι and V′ profiles for M = 4, $R/a_c = 4$ heliacs with and without $\ell = 1$ hardcore winding. For this example, $R_0 = 1$ m, $r_{SW}/a_c = 0.7$, $a_c/a_{hc} = 6$, and $\Delta R/R_0 = 0.0125$.

Variation of the helical hardcore current can also provide a means to vary the shape of the rotational transform profile. Figure 5 shows an example in which the sign of $d\iota/dr$ is changed by varying the fraction of the (fixed) total hardcore current flowing in the helical winding (a heliac without a helical hardcore has $d\iota/dr > 0$). Figure 6 shows similar plots for a configuration having the same pitch but three

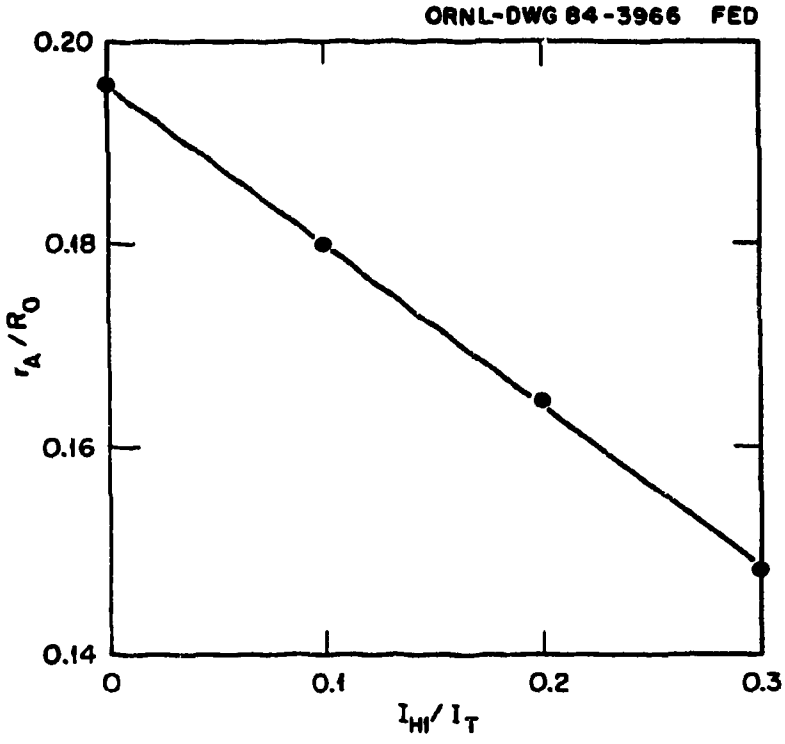

FIG. 4. Magnetic axis position r_A as a function of helical hardcore current I_{H1}/I_T (other parameters as in Fig. 3).

times the aspect ratio and number of field periods. The profiles of ι/M are similar to those in Fig. 5, which indicates that the profile shape is determined directly by helical, rather than toroidal, effects.

A range of possible transform profiles that can be synthesized for a particular configuration is shown in Figs. 7 and 8. In Fig. 7 the fraction of total hardcore current carried by the helical winding is held fixed and the net hardcore current is varied, while in Fig. 8 the net hardcore current is held fixed and the fraction carried by the helical winding is varied. The radius of the last closed flux surface

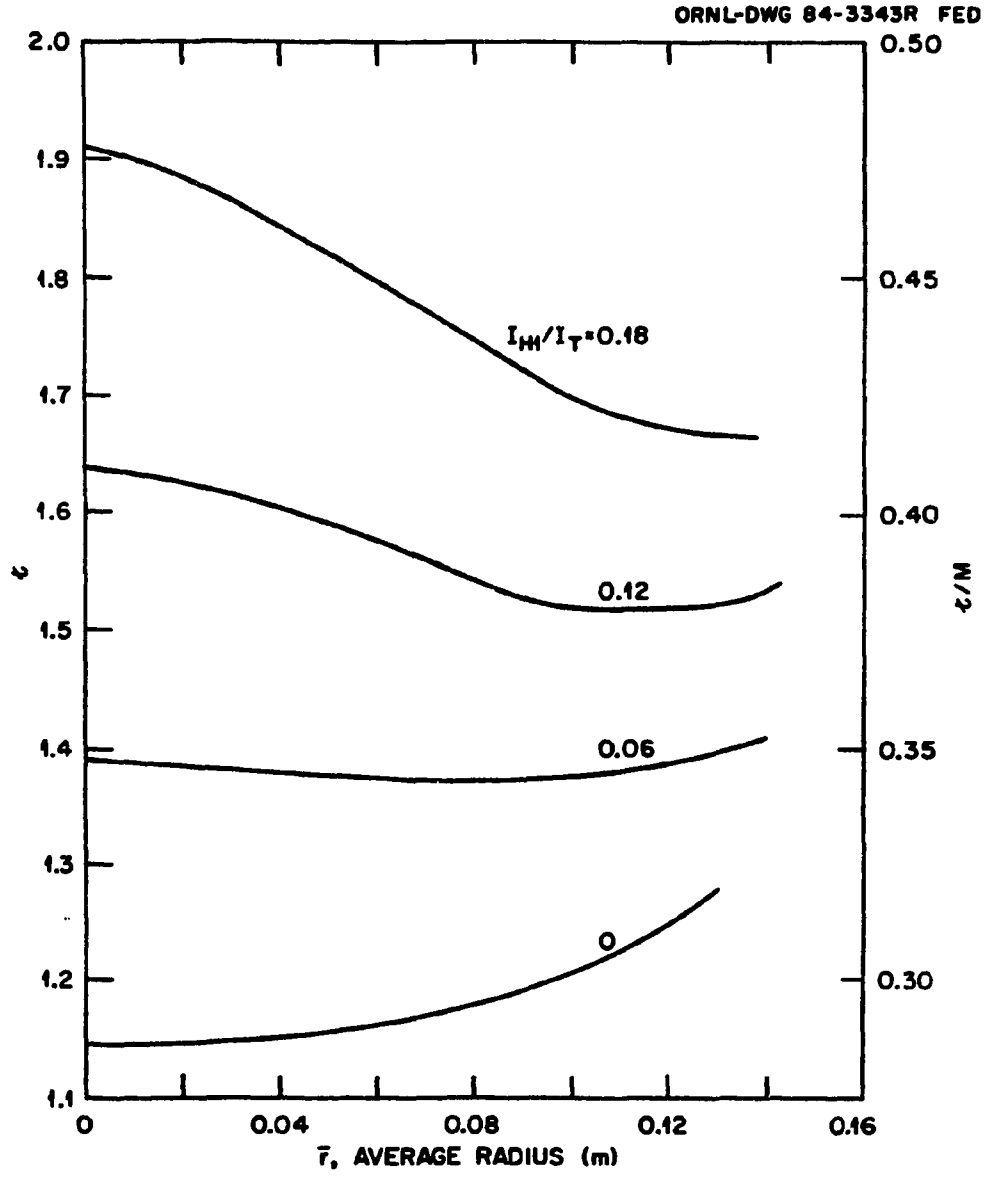

FIG. 5. Effect of increasing helical hardcore current on the ι profile of an $M = 4$, $R/a_c = 4$ heliac. For these calculations, $R_0 = 1$ m, $r_{SW}/a_c = 0.7$, $a_c/a_{hc} = 3.33$, and $I_T/(R_0H_0) = 0.33$.

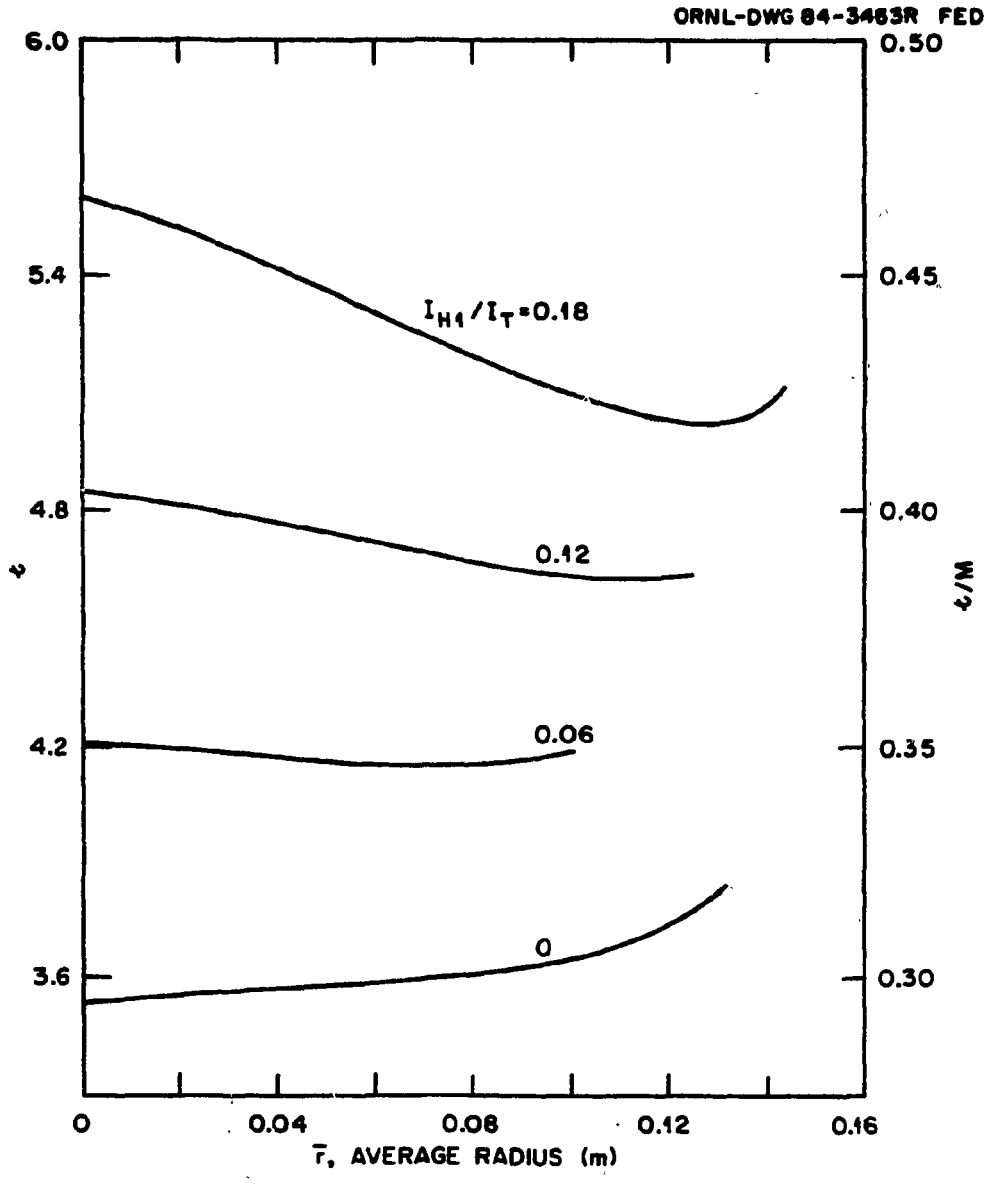

FIG. 6. Effect of increasing helical hardcore current on the ι profile of a heliac with M = 12, R/a_c = 12, and other parameters as in Fig. 4.

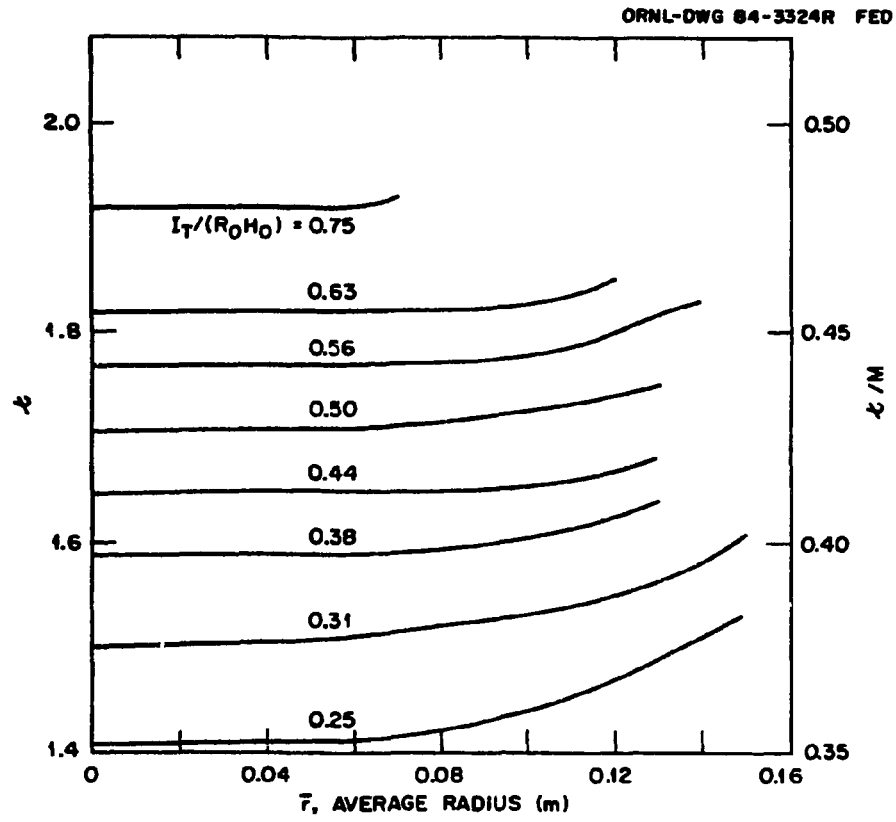

FIG. 7. Rotational transform profiles for a range of net hardcore currents in an M = 4, R/a_c = 4 heliac with a fixed helical hardcore current fraction. I_{H1}/I_T = 0.304 (other parameters as in Fig. 3).

is strongly affected by the proximity of strong resonances (e.g., ι/M = 1/2) that break up the outer flux surfaces, as can be seen in the rotational transform profiles.

Figure 9 shows flux surfaces at two positions within a field period for three configurations from the parameter scans shown in Figs. 7 and 8. The plots illustrate the shapes of the magnetic surfaces obtained for widely varying ι/M values. For the case with the

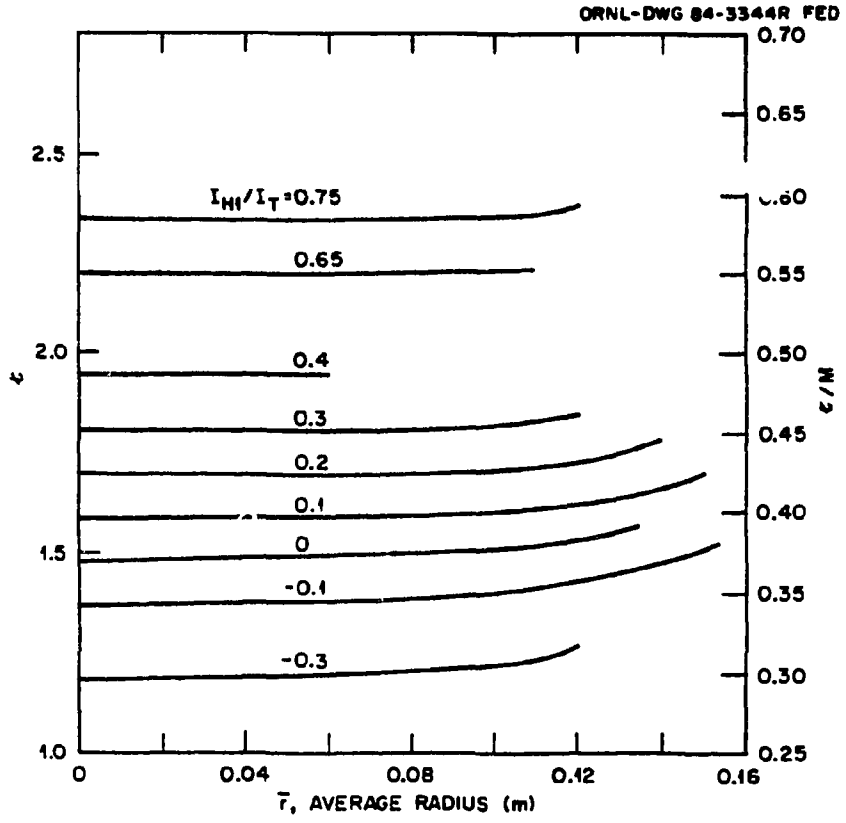

FIG. 8. Rotational transform profiles for a range of helical hardcore current fractions for the configuration of Fig. 7 with fixed net hardcore current $I_T/(R_0H_0) = 0.63$.

rather high value of $\iota_0/M = 0.552$, the magnetic axis has a large helical excursion, and toroidal effects make the surfaces rather asymmetric. This is because the coil parameters of the configuration used for the parameter scan were chosen to give optimum results in the range $\iota/M \lesssim 0.4$. If, for example, the helical excursion of the toroidal field coils (r_{SW}) is reduced to $r_{SW}/a_c \sim 0.5$, the optimum range of ι_0/M shifts upward and highly symmetric surfaces can be obtained with $\iota_0/M > 0.5$.

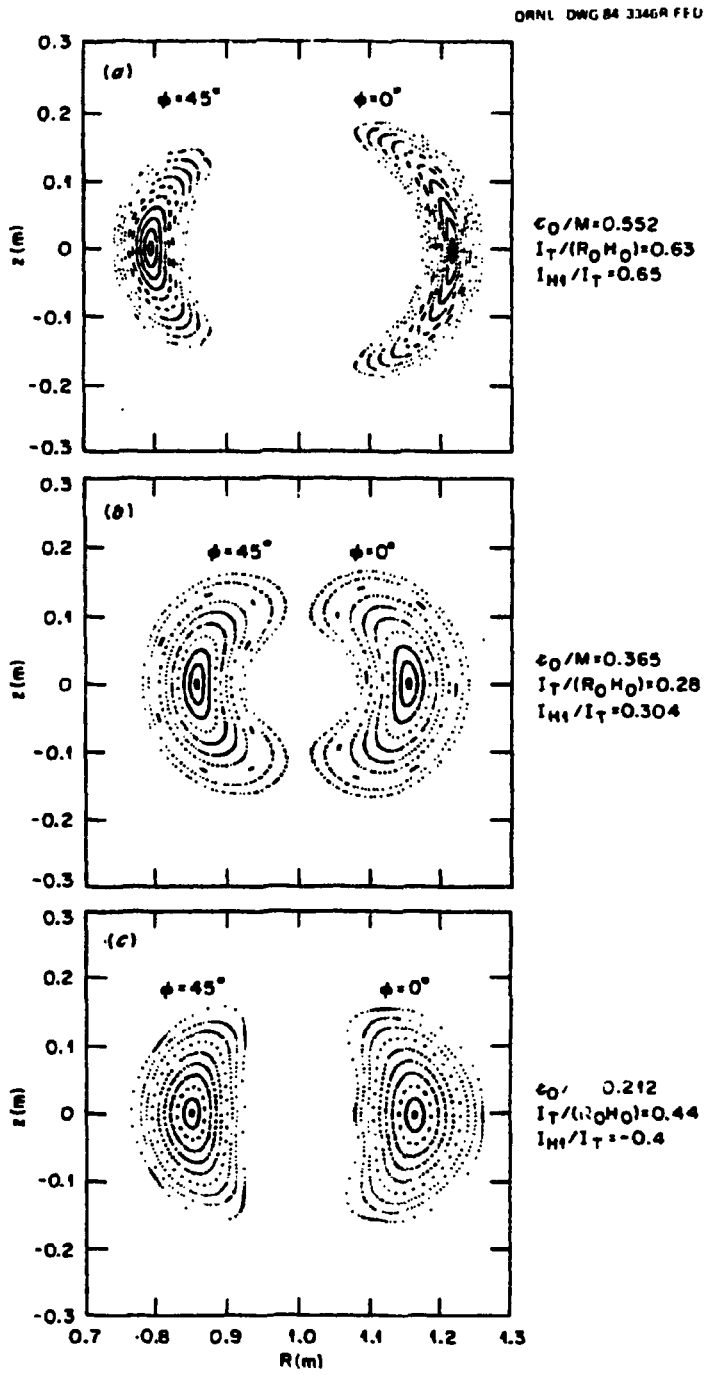

FIG. 9. Flux surfaces at two positions within a field period for heliac configurations of different ε_0/M drawn from the parameter scans shown in Figs. 7 and 8.

We conclude by noting that the range of rotational transform values that can be achieved in an actual device will depend on a careful design of the coil configuration that allows sufficient space for the required windings at realistic current densities. We have carried out preliminary studies of this practical question that indicate that variations in ι/M of at least a factor of about 2 can be readily achieved. Given the large number of design parameters involved, computer optimization techniques [16,17] and concepts for modular heliac coils [18,19] could be profitably applied to further improve modified heliac configurations of the type considered here.

REFERENCES

1. MONTICELLO, D. A., DEWAR, R. L., FURTH, H. P., REIMAN, A., Phys. Fluids 27 (1984) 1248 .
2. MERKEL, P., NÜHRENBERG, J., GRÜBER, R., TROYON, F., Nucl. Fusion 23 (1983) 1061.
3. BAUER, F., BETANCOURT, O., GARABEDIAN, P., Magnetohydrodynamic Equilibrium and Stability of Stellarators, Springer-Verlag, New York (1984).
4. BOOZER, A. H., CHU, T. K., DEWAR, R. L., FURTH, H. P., GOREE, J., JOHNSON, J. L., KULSRUD, R. M., MONTICELLO, D. A., KUO-PETRAVIC, G., SHEFFIELD, G. V., YOSHIKAWA, S., BETANCOURT, O., in Plasma Physics and Controlled Nuclear Fusion Research, Vol. 3, IAEA, Vienna (1983) 129.
5. REIMAN, A., BOOZER, A. H., Phys. Fluids 27 (1984) 2446.
6. LYON, J. F., CARRERAS, B. A., HARRIS, J. H., ROME, J. A., DORY, R. A., GARCIA, L., HENDER, T. C., HIRSHMAN, S. P., JERNIGAN, T. C., SHEFFIELD, J., CHARLTON, L., FOWLER, R. H., HICKS, H. R., HOLMES, J. A., LYNCH, V. E., MASDEN, B. F., GOODMAN, D. L., HOKIN, S. A., in Plasma Physics and Controlled Nuclear Fusion Research, Vol. 3, IAEA, Vienna (1983) 115.
7. CARRERAS, B. A., CANTRELL, J. L., CHARLTON, L. A., GARCIA, L., HARRIS, J. H., HENDER, T. C., HICKS, H. R., HOLMES, J. A., ROME, J. A., LYNCH, V. E., to be published in Plasma Physics and Controlled Nuclear Fusion Research, IAEA, Vienna (1985).

8. WENDELSTEIN VII-A TEAM et al., Plasma Phys. and Controlled Fusion 26 (1984) 183.

9. DANILKIN, I. S., SHPIGEL, I. S., Tr. Fiz. Inst. Akad. Nauk SSSR 65 (1973) 50.

10. FURTH, H. P., KILLEEN, J., ROSENBLUTH, M. N., COPPI, B., in Plasma Physics and Controlled Nuclear Fusion Research, Vol. 1, IAEA, Vienna (1966) 103.

11. MCNAMARA, B., WHITEMAN, K. J., TAYLOR, J. B., in Plasma Physics and Controlled Nuclear Fusion Research, Vol. 1, IAEA, Vienna (1966) 145.

12. ZUEVA, N. M., SOLOV'EV, L. S., Plasma Phys. 8 (1966) 765.

13. YOSHIKAWA, S., Nucl. Fusion 23 (1983) 667.

14. PORITSKY, H., J. Appl. Phys. 30 (1959) 1828.

15. CARY, J., Phys. Fluids 27 (1984) 119.

16. CHODURA, R., DOMMASCHK, W., HERRNEGGER, F., LOTZ, W., NÜHRENBERG, J., SCHLÜTER, A., IEEE Trans. Plasma Sci. 9 (1981) 221.

17. BUTCHER-EHRHARDT, A., in Proc. 5th Int. Stellarator Workshop, Tegernsee, West Germany, EUR-9618EN (1984) 717.

18. REIMAN, A., BOOZER, A. H., Phys. Fluids 26 (1983) 496.

19. HARMEYER, E., KISSLINGER, J., RAU, F., WOBIG, H., to be published in Plasma Physics and Controlled Nuclear Fusion Research, IAEA, Vienna (1985).

ORNL/TM-9504
Dist. Category UC-20 g

INTERNAL DISTRIBUTION

1. J. L. Cantrell
2–5. B. A. Carreras
6. R. A. Dory
7. J. L. Dunlap
8. L. Garcia
9–13. J. H. Harris
14. T. C. Hender
15. H. R. Hicks
16. J. A. Holmes
17. V. E. Lynch
18–21. J. F. Lyon
22. R. N. Morris
23. Y-K. M. Peng
24. J. A. Rome
25. J. Sheffield
26. D. Sigmar
27–28. Laboratory Records Department
29. Laboratory Records, ORNL-RC
30. Document Reference Section
31. Central Research Library
32. Fusion Energy Division Library
33–34. Fusion Energy Division Publications Office
35. ORNL Patent Office

EXTERNAL DISTRIBUTION

36. Office of the Assistant Manager for Energy Research and Development, U.S. Department of Energy, Oak Ridge Operations, Box E, Oak Ridge, TN 37831
37. J. D. Callen, Department of Nuclear Engineering, University of Wisconsin, Madison, WI 53706
38. R. W. Conn, Department of Chemical, Nuclear, and Thermal Engineering, Boelter Hall, University of California, Los Angeles, CA 90024
39. S. O. Dean, Director, Fusion Energy Development, Science Applications, Inc., 2 Professional Drive, Suite 249, Gaithersburg, MD 20760
40. H. K. Forsen, Bechtel Group, Inc., Research & Engineering, P.O. Box 3965, San Francisco, CA 94119
41. R. W. Gould, Department of Applied Physics, California Institute of Technology, Pasadena, CA 91125
42. D. G. McAlees, Exxon Nuclear Company, Inc., 2101 Horn Rapids Road, Richland, WA 99352
43. H. P. Furth, Princeton Plasma Physics Laboratory, P.O. Box 451, Princeton, NJ 08544
44. W. M. Stacey, Jr., Georgia Institute of Technology, School of Nuclear Engineering, Atlanta, GA 30332
45. G. A. Eliseev, I. V. Kurchatov Institute of Atomic Energy, P.O. Box 3402, 123182 Moscow, U.S.S.R.
46. V. A. Glukhikh, Scientific-Research Institute of Electro-Physical Apparatus, 188631 Leningrad, U.S.S.R.
47. I. Shpigel, Institute of General Physics, U.S.S.R. Academy of Sciences, Ulitsa Vavilova, 38, 117924 Moscow, U.S.S.R.
48. D. D. Ryutov, Institute of Nuclear Physics, Siberian Branch of the Academy of Sciences of the U.S.S.R., Sovetskaya St. 5, 630090 Novosibirsk, U.S.S.R.
49. V. T. Tolok, Kharkov Physical-Technical Institute, Academical St. 1, 310108 Kharkov, U.S.S.R.
50. R. Varma, Physical Research Laboratory, Navrangpura, Ahmedabad, India
51. Bibliothek, Max-Planck-Institut fur Plasmaphysik, D-8046 Garching bei Munchen, Federal Republic of Germany

52. Bibliothek, Institut fur Plasmaphysik, KFA, Postfach 1913, D-5170 Julich, Federal Republic of Germany
53. Bibliotheque, Centre de Recherches en Physique des Plasmas, 21 Avenue des Bains, 1007 Lausanne, Switzerland
54. Bibliotheque, Service du Confinement des Plasmas, CEA, B.P. No. 6, 92 Fontenay-aux-Roses (Seine), France
55. Documentation S.I.G.N., Department de la Physique du Plasma et de la Fusion Controlee, Association EURATOM-CEA, Centre d'Etudes Nucleaires, B.P. 85, Centre du Tri, 38041 Cedex, Grenoble, France
56. Library, Culham Laboratory, UKAEA, Abingdon, Oxfordshire, OX14 3DB, England
57. Library, FOM Instituut voor Plasma-Fysica, Rijnhuizen, Jutphaas, The Netherlands
58. Library, Institute of Physics, Academia Sinica, Beijing, Peoples Republic of China
59. Library, Institute for Plasma Physics, Nagoya University, Nagoya 64, Japan
60. Library, International Centre for Theoretical Physics, Trieste, Italy
61. Library, Laboratorio Gas Ionizzati, Frascati, Italy
62. Library, Plasma Physics Laboratory, Kyoto University, Gokasho Uji, Kyoto, Japan
63. Plasma Research Laboratory, Australian National University, P.O. Box 4, Canberra, ACT 2000, Australia
64. Thermonuclear Library, Japan Atomic Energy Research Institute, Tokai, Naka, Ibaraki, Japan
65. D. Steiner, Rensselaer Polytechnic Institute, Troy, NY 12181
66. J. F. Clarke, Associate Director for Fusion Energy, Office of Energy Research, Mail Station G-256, Office of Fusion Energy, U.S. Department of Energy, Washington, DC 20545
67. D. B. Nelson, Acting Director, Division of Applied Plasma Physics, Office of Fusion Energy, Office of Energy Research, Mail Stop G-256, U.S. Department of Energy, Washington, DC 20545
68. M. N. Rosenbluth, RLM 11.218, Institute for Fusion Studies, University of Texas, Austin, TX 78712
69. W. Sadowski, Fusion Theory and Computer Services Branch, Office of Fusion Energy, Office of Energy Research, Mail Stop G-256, U.S. Department of Energy, Washington, DC 20545
70. W. R. Ellis, Mirror Systems Branch, Office of Fusion Energy, Office of Energy Research, Mail Stop G-256, U.S. Department of Energy, Washington, DC 20545
71. J. M. Turner, Mirror Systems Branch, Office of Fusion Energy, Office of Energy Research, Mail Stop G-256, U.S. Department of Energy, Washington, DC 20545
72. J. Cowles, Mirror Systems Branch, Office of Fusion Energy, Office of Energy Research, Mail Stop G-256, U.S. Department of Energy, Washington, DC 20545
73. Theory Department Read File, c/o D. W. Ross, Institute for Fusion Studies, University of Texas at Austin, Austin, TX 78712
74. Theory Department Read File, c/o R. C. Davison, Director, Plasma Fusion Center, 167 Albany Street, Cambridge, MA 02139
75. Theory Department Read File, c/o F. W. Perkins, Princeton Plasma Physics Laboratory, P.O. Box 451, Princeton, NJ 08544
76. Theory Department Read File, c/o L. Kovrizhnykh, Institute of General Physics, U.S.S.R. Academy of Sciences, Ulitsa Vavilova, 38, 117924 Moscow, U.S.S.R. V312
77. Theory Department Read File, c/o B. B. Kadomtsev, I. V. Kurchatov Institute of Atomic Energy, P.O. Box 3402, Moscow, U.S.S.R. 123182
78. Theory Department Read File, c/o T. Kamimura, Institute of Plasma Physics, Nagoya University, Nagoya Japan
79. Theory Department Read File, c/o C. Mercier, Euratom-CEA, Service de Recherches sur la Fusion Controlee, Fontenay-aux-Roses (Seine), France
80. Theory Department Read File, c/o T. E. Stringer, JET Joint Undertaking, Culham Laboratory, Abingdon, Oxfordshire, OX14 3DB, England
81. Theory Department Read File, c/o K. Roberts, Culham Laboratory, Abingdon, Oxon, OX14 3DB, England

82. Theory Department Read File, c/o D. Biskamp, Max-Planck-Insitut fur Plasmaphysik, D-8046 Garching bei Munchen, Federal Republic of Germany
83. Theory Department Read File, c/o T. Takeda, Japan Atomic Energy Research Institute, Tokai, Naka, Ibaraki, Japan
84. Theory Department Read File, c/o C. S. Liu, GA Technologies, Inc., P.O. Box 81608, San Diego, CA 92138
85. Theory Department Read File, c/o L. D. Pearlstein, Lawrence Livermore National Laboratory, P.O. Box 808, Livermore, CA 94550
86. Theory Department Read File, c/o R. Gerwin, CTR Division, MS 640, Los Alamos National Laboratory, P.O. Box 1663, Los Alamos, NM 87545
87. R. E. Mickens, Atlanta University, Department of Physics, Atlanta, GA 30314
88. J. R. Gilleland, GA Technologies, Inc., Fusion and Advanced Technology, P.O. Box 85608, San Diego, CA 92138
89. R. A. Gross, Plasma Research Laboratory, Columbia University, New York, NY 10027
90. D. M. Meade, Plasma Physics Laboratory, Princeton University, P.O. Box 451, Princeton, NJ 08544
91. P. J. Reardon, Brookhaven National Laboratory, Upton, NY 11973

92–250. Given distribution as shown in TID-4500, Magnetic Fusion Energy (Category Distribution UC-20 g: Theoretical Plasma Physics)